屈服强度参数对 10Ni5CrMoV钢焊接残余应力数值计算结果的影响

张　晓[1]，　姚润钢[1]，　王任甫[1]，　薛　钢[1]，　杨建国[2]
（1. 中国船舶重工集团公司 第七二五研究所，河南 洛阳　471039；
2. 哈尔滨工业大学 现代焊接生产技术国家重点实验室，哈尔滨　150001）

摘　要：为了研究低合金高强钢在焊接过程中屈服强度参数变化对焊接数值计算结果的影响，测定了在稳态和冷却条件下 10Ni5CrMoV钢在不同温度时的屈服强度和焊接接头的焊接残余应力，并采用有限元软件分别根据两种条件下所测屈服强度参数对 10Ni5CrMoV钢焊接接头的焊接残余应力进行了数值计算．结果表明，冷却条件下不同温度的屈服强度测试值低于稳态条件下相应温度屈服强度测定值，根据冷却条件下测定的屈服强度曲线计算所得焊接残余应力分布与实测值具有更好的吻合度．

关键词：屈服强度；残余应力；数值计算
中图分类号：TG44　　文献标识码：A　　文章编号：0253－360X（2010）04－0097－04

张　晓

0　序　　言

对焊接残余应力和变形的数值计算研究是近年来焊接研究领域的热点，国内外大量的学者对此进行了广泛研究[1-4]．但是目前的研究主要集中在焊接计算模型的改进与优化、计算效率的提高以及对具体焊接条件下数值计算过程的实现等方面，而材料参数对数值计算结果的影响则未引起足够的重视．实际上反应焊接过程中材料状态的各种材料参数的准确测定是决定焊接残余应力数值计算结果准确与否的前提条件[5-7]．目前计算所采用的材料参数，大多数均是在稳态条件下测定的，但是焊接过程是一个快速加热和冷却的非稳态过程，因此不同情况下测定的材料参数必然存在一定的差别，尤其对于低合金高强钢，在焊接过程中会发生复杂的相变，从而影响到其材料物理参数．文中通过试验方法分别测定了稳态和冷却条件下 10Ni5CrMoV钢不同温度下的屈服强度，并研究了两者对焊接残余应力数值计算结果的影响．

1　试验方法

试验材料为室温屈服强度大于 785 MPa级的 10Ni5CrMoV钢．在 INSTRON5507型材料试验机上测定该钢稳态和空冷条件下不同温度的屈服强度．稳态试验条件为采用加热炉加热到试验温度，保温一段时间后进行拉伸试验；冷却试验条件为先将试样加热至 1 000 ℃，后空冷至试验温度进行拉伸试验．

分别采用上述试验获得的两套屈服强度参数进行 10Ni5CrMoV钢焊接残余应力的数值计算，并与实际焊接试板残余应力测试值进行比较．焊接试板采用平板对接试板，试板尺寸为 250 mm×300 mm×16 mm，在试板上开 60°双 V形坡口，用与 10Ni5CrMoV钢相配套的焊条电弧焊焊接．用 2904-A1型 X射线应力仪对焊接残余应力进行测试，具体残余应力测试位置如图 1所示．

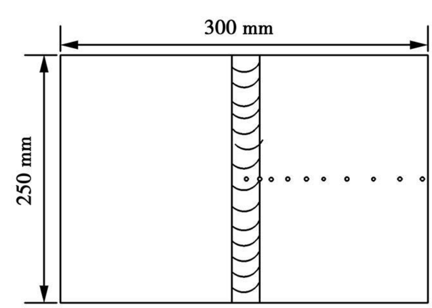

图 1　残余应力测试位置分布
Fig. 1　Measurement position distribution of residual stress

收稿日期：2008－12－01

2 试验结果

稳态和冷却条件下测定的 10Ni5CrMoV钢屈服强度与温度的关系如图 2所示. 在室温与 700 ℃的温度区间内,冷却条件下测定的各温度的屈服强度要远小于稳态条件下的测定值.

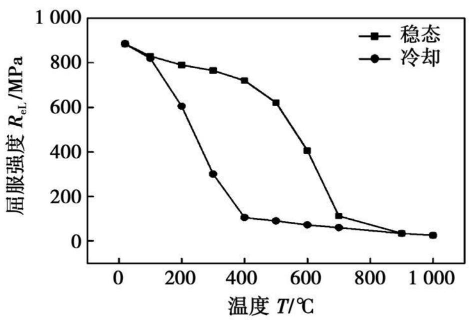

图 2 10Ni5CrMoV钢屈服强度与温度关系
Fig. 2 Variation of yield strength with temperature of 10Ni5CrMoV steel

焊接残余应力的测试结果如图 3所示, 纵向残余应力在焊缝和焊趾部位高达 450 MPa,横向残余应力在焊缝中心部位为 −110 MPa,在焊趾部位高达 200 MPa,可以看出高的残余应力只集中在距焊缝中心 15 mm范围内, 这说明高强钢在焊接过程中只有很窄的范围内发生了塑性变形, 符合高强钢的焊接特点.

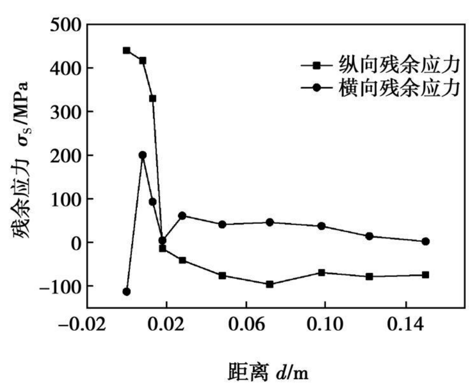

图 3 残余应力测试结果
Fig. 3 Measured results of residual stress

3 焊接残余应力数值分析

3.1 建模与边界条件

焊接残余应力的数值计算采用 MSC.MARC软件进行, 按实际焊接试板形状与尺寸建立如图 4所示的有限元模型, 该模型采用八节点六面体实体正方体单元划分网格, 在靠近焊缝处网格划分相应加密.

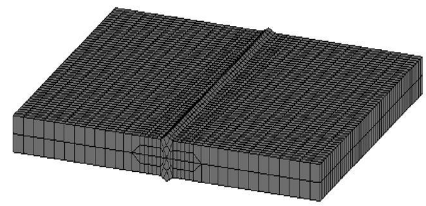

图 4 有限元计算模型
Fig. 4 Finite element model

计算中的边界条件包括温度场分析的边界条件和应力应变分析的边界条件, 因此共施加了 3种边界条件.

(1) 位移边界条件. 在控制刚体位移的同时保证模型在焊接过程中能自由伸缩变形, 具体如图 5所示, P_1 点固定 x和 y方向的位移, P_2 点固定 y和 z方向的位移, 考虑到模型的对称性在 P_1 和 P_2 对称位置节点也施加同样的位移.

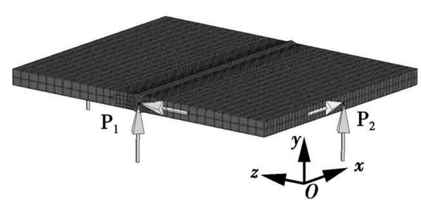

图 5 位移边界条件
Fig. 5 Mechanical boundary condition

(2) 换热边界条件. 焊件的边界与周围介质主要通过对流和辐射两种方式换热, 此处将辐射换热与对流换热通过一个总的换热系数一起考虑, 边界换热损失的热能表示为

$$q = q_c + q_r = (\alpha_c + \alpha_r)(T - T_0) = \alpha(T - T_0)$$

式中: T为焊接温度; T_0 为环境温度; α为全部表面放热系数, 等于对流和辐射换热系数之和; q_c 为通过对流方式换热损失的热量; q_r 为通过辐射方式换热损失的热量.

(3) 焊接热源边界条件. 目前常用的热源模型是高斯热源和双椭球热源. 对于平板堆焊和对接焊, 常采用高斯热源来模拟. 对于开坡口的对接焊或者熔深较大时, 可以采用双椭球热源模型, 文中采用双椭球热源. 双椭球热源模型的前后两部分采用不同的表达式, 前半部分椭球内热源分布的表达式

为[8]

$$q(x,y,z)=\frac{6\sqrt{3}f_1Q}{\pi a_1 bc\sqrt{\pi}}\exp\left(-3\frac{x^2}{a_1^2}\right)\exp\left(-3\frac{y^2}{b^2}\right)\exp\left(-3\frac{z^2}{c^2}\right)$$

后半部分椭球内热源分布的表达式为

$$q(x,y,z)=\frac{6\sqrt{3}f_2Q}{\pi a_2 bc\sqrt{\pi}}\exp\left(-3\frac{x^2}{a_2^2}\right)\exp\left(-3\frac{y^2}{b^2}\right)\exp\left(-3\frac{z^2}{c^2}\right)$$

式中:$Q=\eta UI$,η为热源效率,U为电弧电压(V),I为焊接电流(A);$f_1=0.6$,$f_2=1.4$,表示电弧前端和后端能量分配系数[9];a_1,a_2,b,c分别为椭球形状参数;x,y,z分别为三个坐标方向.根据实际焊接条件在计算中打底焊道采用小热输入参数焊接,最后一条焊道采用大热输入参数焊接,具体的参数值如表 1所示.

表 1　热源参数

Table 1　Parameters of heat source

热输入	热源前长 a_1/mm	热源后长 a_2/mm	热源熔宽 b/mm	热源熔深 c/mm
小	2.4	2.4	10.5	2.2
大	7.2	7.2	14.0	2.3

目前的大型有限元结构分析软件在计算焊接温度场分布时不能直接计算熔池中的液体对流和凝固,例如 ANASYS,ABAQUS和 MARC等,这是因为在目前版本的软件中固态和液态耦合问题不能直接解决;但是熔池中的液态对流对焊接温度场和熔池形貌形成有很大的影响,如果液体对流被忽略,熔池中的最高温度将会非常的高.当采用高斯双椭球热源计算时,最高温度将超过 3 000 ℃. Okagaito等人[10]测定了 SUS304钢 TIG焊熔池表面温度最高温度大概是 1 750 ℃.文中计算为了考虑熔池中的对流,加大了熔池的热传导系数.当有限元节点的温度超过熔点,热传导系数设定为室温的两倍,此时计算所获得熔池表面温度为 1 700 ℃,这同实际的情况更为接近.考虑相变潜热值比较小,在计算时未考虑相变潜热的影响[11].

假设材料各向同性,泊松比为 0.285,质量密度为 7 800 kg/m³,其余随温度变化的材料性能均是通过稳态加热所获得,具体如图 6所示.

3.2　计算结果与分析

根据不同试验条件测定的屈服强度参数进行的焊接残余应力值如图 7所示.

两种条件下计算所得焊接残余应力分布趋势与实测值基本一致:焊缝和焊趾部位存在较高的纵向拉应力,如图 7所示;横向拉应力峰值则出现在

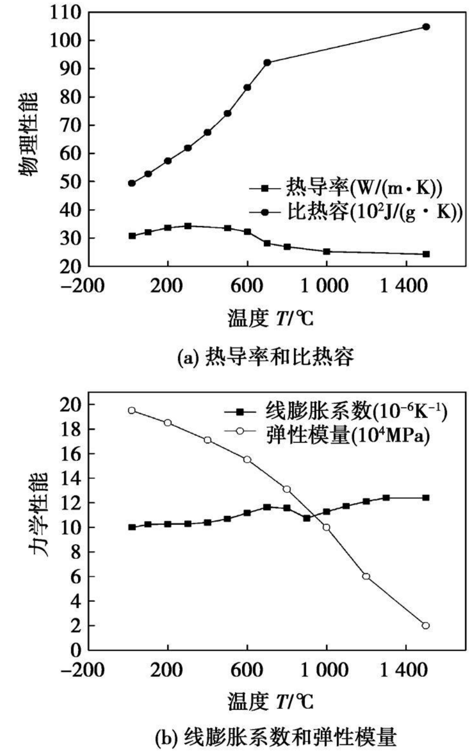

(a) 热导率和比热容

(b) 线膨胀系数和弹性模量

图 6　10Ni5CrMoV钢材料性能

Fig. 6　Thermo-mechanical properties of 10Ni5CrMoV steel

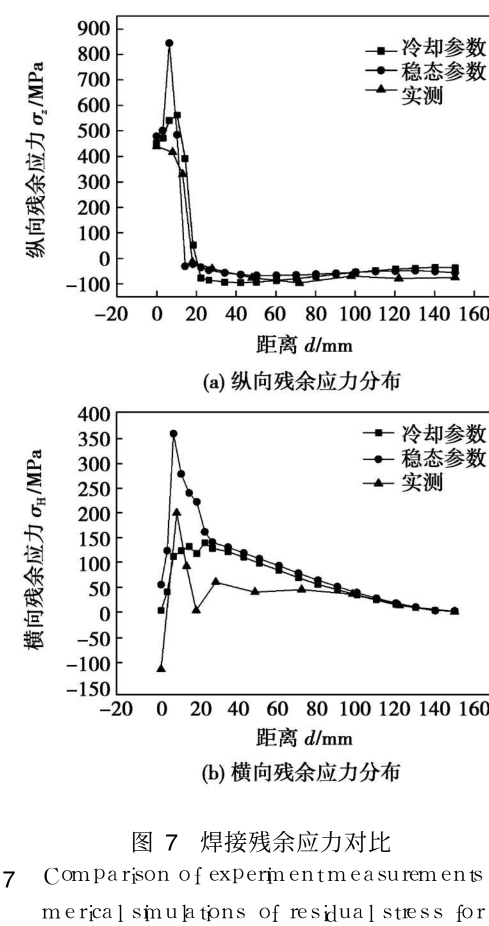

(a) 纵向残余应力分布

(b) 横向残余应力分布

图 7　焊接残余应力对比

Fig. 7　Comparison of experiment measurements and numerical simulations of residual stress for different yield stress

焊趾部位,如图 7 b所示. 不同屈服强度参数对计算结果的影响主要体现在应力值的大小: 采用稳态屈服强度参数计算所得的各点应力值较高, 纵向残余拉应力峰值达到 840 MPa,接近材料的室温屈服强度, 远高于实测 440 MPa;横向残余拉应力峰值为 360 MPa,也高于实测值. 采用冷却条件屈服强度参数计算所得各点应力值则相对较低, 纵向残余应力峰值为 560 MPa,横向残余应力峰值为 130 MPa,均与实测值吻合较好.

4 分析与讨论

低合金高强钢在焊接热循环过程发生的相变对于它的力学性能会产生很大的影响, 对于屈服强度来说和加热过程的屈服强度降低相比, 在冷却转变成两相材料时屈服极限降低的更多. 这种现象会对残余应力的形成产生很大的影响, 特别是对于焊缝金属和与其相邻的热影响区, 这种影响更大. 这主要是因为对于焊缝金属以及与其相邻的热影响区来说, 由于其瞬时达到超过 1 000 ℃高温, 金属的物性和状态几乎全部消失, 所以就应力和变形的分析而言, 可以认为并不存在加热过程, 只有冷却阶段. 在冷却过程中的计算如果还是采用在加热过程的材料参数, 高的屈服强度参数会增大热源周围材料的内拘束度, 这会增大残余应力的计算结果. 采用冷却的参数即较低的屈服强度参数, 相对更为符合实际焊接过程中的材料性能变化, 因此采用与实际更吻合的冷却阶段屈服强度变化参数能获得更吻合的结果.

实际上屈服强度只是决定数值结果准确性的一个重要因素, 材料在加热和冷却过程线膨胀系数也是影响数值计算结果准确性的重要因素[5,7,8]. 由于实际试验条件的限制, 很难在试验中测得冷却过程中线膨胀系数的变化. 在文中的计算中, 线膨胀系数仍然采用稳态加热过程中所获得数据, 因此在计算焊接应力应变情况时仍有一定的误差. 在下一步的工作中需要综合考虑相变所引起的屈服强度和线膨胀系数变化对焊接残余应力的影响.

5 结 论

(1) 不同条件下测定 10Ni5CrMoV钢的屈服强度存在很大差别, 冷却条件下测定的屈服强度要远低于稳态.

(2) 材料参数的选择对焊接残余应力数值分析准确性有重要影响, 屈服强度参数对于应力计算有着重要的影响, 在计算中必须考虑屈服强度参数的变化才能获得正确的结果. 文中采用与实际焊接状况相较为接近的冷却条件下测定的屈服强度参数所获得的计算结果与实测结果吻合较好.

参考文献:

[1] Tekriwal P, Mazumder J. Transient and residual thermal strain-stress analysis of GMAW[J]. Materials Technology, 1991, 113(36): 338−343

[2] 胡军峰, 方洪渊, 杨建国. 电弧摆动对焊接应力场的影响[J]. 焊接学报, 2007, 28(1): 65−68
Hu Junfeng, Fang Hongyuan, Yang Jianguo. Influence of arc weaving on welding residual stress field[J]. Transactions of the China Welding Institution, 2007, 28(1): 65−68.

[3] Fricke S, Keim E, Schmidt J. Numerical weld modeling-a method for calculating weld-induced residual stresses[J]. Nuclear Engineering and Design, 2001, 206(45): 139−150

[4] 鹿安理, 史清宇, 赵海燕. 厚板焊接过程温度场、应力场的三维有限元数值模拟[J]. 中国机械工程, 2001, 13(2): 183−186.
Lu Anli, Shi Qingyu, Zhao Haiyan. Three dimensional numerical simulation of temperature and stress distribution in welding of thick plate[J]. China Mechanical Engineering, 2001, 13(2): 183−186

[5] Dean D, Hidekazu M. Prediction of welding residual stress in multi-pass butt welded modified 9Cr-1Mo steel pipe considering phase transformation effects[J]. Computational Materias Science, 2006, 112(37): 209−219.

[6] Lidgren L E. Finite element modeling and simulation of welding (part II): improved material modeling[J]. Therm Stress, 2001, 132(24): 195−231.

[7] Masubuchi K. Analysis of welded structures[M]. Oxford, UK: Pergamon Press, 1980

[8] Zhu X K, Chao Y J. Effects of temperature-dependent material properties on welding simulation[J]. Computers and Structures, 2002, 165(80): 967−976

[9] Goldak J, Chakravarti A, Bibby M. A new finite model for welding heat sources[J]. Metallurgical Transactions B, 1984, 28(15): 299−305

[10] Okagaito T, Ohji T, Miyasaka F. UV radiation thermometry of TIG weld pool development of UV radiation thermoetry (report 1)[J]. Journal of the Japan Welding Society, 2004, 22(1): 21−6

[11] 赵 明, 武传松, 陈茂爱. 焊接热过程数值分析中相变潜热的三种解决方案[J]. 焊接学报, 2006, 27(9): 55−58.
Zhao Ming, Wu Chuansong, Chen Maoai. Solutions for latent heat of phase change in numerical analysis of arc welding[J]. Transactions of the China Welding Institution, 2006, 27(9): 55−58.

作者简介: 张 晓, 男, 1983年出生, 硕士. 主要从事焊接数值模拟和焊接材料工作. 发表论文 3篇.
Email: zhang_xiao08@163.com

miniaturized workpiece of dissimilar metal, the joins of iron wire to copper sheet were obtained by using process of condenser discharge percussion welding successfully. The effects of process parameters, namely capacitance, charging voltage, wire taper angle and machine oil, on fracture pull of the joint were studied. Meanwhile, the microstructure of the joint was analyzed with optical microscope and SEM. The results show that condenser discharge percussion welding is suitable for joining iron wire to copper sheet. The maximum fracture pull of the joint can reach to 350 N, and fusion zone close to wire taper is composed of fine grains which sizes are 2 to 8 μm. The optimum parameters are obtained at 60 mF capacitance, 68 V charging voltage, 50° wire taper angle and added machine oil.

Key words: condenser discharge percussion welding; iron wire and copper sheet; fracture pull; microstructure

Effects of yield strength parameters on welding residual stress simulation results of 10Ni5CrMoV steel ZHANG Xiao[1], YAO Rungang[1], WANG Renfu[1], XUE Gang[2], YANG Jianguo[2] (1. Luoyang Ship Materials Research Institute, Luoyang 471039, China; 2. State Key Laboratory of Advanced Welding Production Technology, Harbin Institute of Technology, Harbin 150001, China). p 97—100

Abstract: Experiments were carried out to determine yield strength of 10Ni5CrMoV steels in stable heating and air-cooling process, and effects on residual stress of the yield strength change due to solid-state phase transformation in butt welded joints of 10Ni5CrMoV steels were investigated by means of numerical techniques. The simulated results show that the temperature-dependent yield strength has great influences on the welding residual stress, the yield strength of the joint in the air cooling cases is lower than that in the stable temperature case due to phase transformation, and the distribution of the simulated weld residual stress is generally in good agreement with the experimental results.

Key words: yield strength; residual stress; numerical simulation

Microstructure and fractography of intermediate frequency spot welding of precision ultra-high strength quenching steel HAN Lijun[1], GU Zhengwei[2], ZHANG Zhenglin[2] (1. The FAW-Volkswagen Automobile Company Ltd., Changchun 130011, China; 2. College of Materials Science and Engineering, Jilin University, Changchun 130022, China). p 101—104

Abstract: Precision ultra-high strength quenching steel EN10292 TL4225 was selected for the study. The intermediate frequency (IF) spot welding process, one kind of advanced jointing technologies, was used, and the perfect welded joints were obtained by using the optimum welding parameters. The mechanical properties of the joints, such as the tension strength, the hardness distribution, were tested, and the microstructure of the fracture was analyzed by scanning electron microscope. The test results show that the joints welded by using IF spot welding process has good mechanical properties, the microstructure of the joints is similar with that of the base metal, the fracture of the joints has the characteristics of plastic, and the mechanical properties completely meet the actual need of car product crash test and road testing.

Key words: precision ultra-high strength steel; intermediate frequency spot welding; mechanical properties; microstructure

A double-characteristic fusion-control algorithm for resistance spot welding GUO Haibin, LI Guizhong (School of Materials Science and Engineering, Jilin University, Changchun 130025, China). p 105—108

Abstract: On the basis of the co-control strategies, the algorithm of heat regulation is optimized for resistance spot welding by use of fuzzy control and single-chip computer technology. The monitoring mode of double-characteristics, dynamic current lag angle characteristic and dynamic current characteristic, is set up, and then the twice fuzzy decision-making method with multi-information fusion technology is applied in monitoring information, such as current lag angle incremental deviation e_n, heat percentage adjustment increment $\triangle m_n$ in present cycle, heat percentage adjustment increment $\triangle m_{n+1}$ in next cycle and welding current deviation $\triangle I_n$ in present cycle. The results prove that this monitoring mechanism not only can be better control the direction and scale of heat regulation, but also can ensure the consistency of the quality of welding nugget and welding time.

Key words: resistance spot welding; double-characteristic monitoring mode; multi-information fusion; twice-fuzzy decision-making method

Influence of nodulizer type on quality of BGA solder ball GUO Xiaoxiao[1,2], YAN Yanfu[1,2], FENG Lifang[1], ZHAO Tian[1] (1. School of Materials Science and Engineering, Henan University of Science and Technology, Luoyang 471003, China; 2. Henan Key Laboratory of Advanced Non-ferrous Metals, Henan University of Science and Technology, Luoyang 471003, China). p 109—112

Abstract: Solder ball is the key material of the bump fabrication in the BGA and μBGA high integrated package, and the nodulizer type is the main factor which affects the quality of the solder balls. The solder ball is fabricated by the fine wire cutting-remelting method when preheating temperature is 500 centidegree and spheroidization temperature is 280 centidegree, and arachis oil, silicone oil, heavy oil and engine oil are selected as nodulizers respectively. The influences of the different nodulizers on the real sphericity and the surface appearance of the 63Sn37Pb solder ball are investigated. Results show that the real sphericity value of the 63Sn37Pb solder ball is the smallest and the shape of the solder ball is more like true sphere. At the same time, the surface appearance of the solder ball is the best when the arachis oil is used as the nodulizer. The quality of solder ball is the worst when the engine oil is used as the nodulizer, and the qualities of solder balls are between them when heavy oil and silicon oil are used as the nodulizer respectively.

Key words: solder ball; fine wire cutting-remelting; nodulizer type; real sphericity; surface appearance